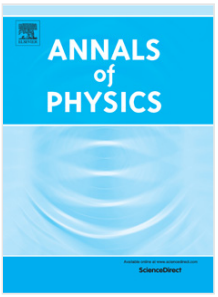

Higher-order Dirac solitons in binary waveguide arrays

Truong X. Tran, Dũng C. Duong

PII: S0003-4916(15)00280-8
DOI: http://dx.doi.org/10.1016/j.aop.2015.07.015
Reference: YAPHY 66899

To appear in: *Annals of Physics*

Received date: 31 January 2015
Accepted date: 18 July 2015

Please cite this article as: T.X. Tran, D.C. Duong, Higher-order Dirac solitons in binary waveguide arrays, *Annals of Physics* (2015), http://dx.doi.org/10.1016/j.aop.2015.07.015

Highlights of *"Higher-order Dirac solitons in binary waveguide arrays"* by Truong X. Tran and Dũng C. Duong

- Higher-order Dirac solitons in nonlinear binary waveguide arrays are numerically demonstrated.
- Amplitude profiles of higher-order Dirac solitons are periodic during propagation.
- The period of higher-order Dirac solitons decreases when the soliton order increases.

Higher-order Dirac solitons in binary waveguide arrays

Truong X. Tran[a,b,1] and Dũng C. Duong[a]

[a] *Dept. of Physics, Le Quy Don University, 236 Hoang Quoc Viet str., 10000 Hanoi, Vietnam*
[b] *Max Planck Institute for the Science of Light, Günther-Scharowsky str. 1, 91058 Erlangen, Germany*

Abstract

We study optical analogues of higher-order Dirac solitons (HODSs) in binary waveguide arrays. Like higher-order solitons obtained from the well-known nonlinear Schrödinger equation governing the pulse propagation in an optical fiber, these HODSs have amplitude profiles which are numerically shown to be periodic over large propagation distances. At the same time, HODSs possess some unique features. Firstly, the period of a HODS depends on its order parameter. Secondly, the discrete nature in binary waveguide arrays imposes the upper limit on the order parameter of HODSs. Thirdly, the order parameter of HODSs can vary continuously in a certain range.

Keywords:
Binary waveguide array; Higher-order Dirac soliton; Kerr nonlinearity; Quantum-optical analogies.

1. Introduction

Waveguide arrays (WAs) have been used intensively to simulate the evolution of a non-relativistic quantum mechanical particle in a periodic potential [1]. Many fundamental phenomena in non-relativistic classical and quantum mechanics such as Bloch oscillations [2, 3] and Zener tunneling [4, 5] have been investigated both theoretically and experimentally by using WAs. It was shown in recent studies that most of nonlinear phenomena usually associated to fiber optics (such as the emission of resonant radiation from

[1] Corresponding author. Tel.: +84-(0)43-6611-581; +84-(0)162-9686-475
E-mail address: truong.tran@mpl.mpg.de

solitons and soliton self-wavenumber shift) can also take place in specially excited WAs, but in the spatial domain rather than in the temporal domain [6, 7]; and the supercontinuum in both frequency and wave number domains can be generated in nonlinear WAs [8]. Binary waveguide arrays (BWAs) have been used to mimic relativistic phenomena typical of quantum field theory, such as Klein tunneling [9, 10], *Zitterbewegung* (trembling motion of a free Dirac electron) [11, 12], and fermion pair production [13], which are all based on the properties of the Dirac equation [14]. The discrete gap solitons in BWAs in the *classical* context have been investigated both numerically [15, 16, 17] and experimentally [18]. Gap and out-gap solitons and breathers in BWAs have been investigated in great detail both analytically and numerically [19, 20, 21]. These gap solitons were already known in [22] in 1992 for diatomic lattices, and later explicitly derived (in their exact continuum-limit form) for the BWA system in [19] in 2011. Recently, the explicit suggestion to use BWAs to simulate a quantum nonlinear Dirac equation has been put forward in [23] where the gap solitons in BWAs have been shown to be connected to Dirac solitons (DSs) in a nonlinear extension of the relativistic one-dimensional (1D) Dirac equation describing the dynamics of a freely moving relativistic particle. Other soliton solutions have been found for the nonlinear 1D Dirac equation [24], but with a different kind of nonlinearity, in the context of quantum field theory. The 1D DS stability, its dynamics and different scenarios of soliton interaction have been systematically investigated in [25]. The formation and dynamics of two-dimensional DSs in square binary waveguide lattices have been investigated in [26]. Although there is currently no evidence for fundamental quantum nonlinearities, nonlinear versions of the Dirac equation have been studied since a long time. One of the earlier extensions was investigated by Heisenberg [27] in the context of field theory and was motivated by the question of mass. In the quantum mechanical context, nonlinear Dirac equations have been used as effective theories in atomic, nuclear and gravitational physics [28, 29, 30, 31]. To this regard, BWAs can offer a unique platform to simulate nonlinear extensions of the Dirac equation when probed at high light intensities. One of these possibilities is to use BWAs as a classical simulator of the Dirac equation to mimic the two-body Dirac model, i.e. the Dirac equation for two interacting relativistic particles, which has attracted interest of researchers since the early days of quantum mechanics [32, 33].

Soliton solutions to the well-known nonlinear Schrödinger equation (NLSE) governing the pulse propagation in an optical fiber have been thoroughly in-

vestigated among various classes of solitons [34, 35, 36]. The shape of the fundamental temporal soliton obtained from the NLSE (further referred to as NLS solitons) is described by the hyperbolic function $u(\tau) = sech(\tau)$. This shape is absolutely retained during propagation of the fundamental NLS soliton along the optical fiber. In light of this, the DS investigated in [23] can also be termed as the fundamental DS, cause its profile is also conserved during propagation along the longitudinal axis of BWAs. However, apart from the fundamental soliton solution, the NLSE also has so-called higher-order (HO) soliton solutions with initial shapes being described by $Nsech(\tau)$ where N is an arbitrary integer provided that $N \geq 2$ [35, 37, 38] (further referred to as HONLS solitons). Unlike the fundamental NLS soliton, HONLS solitons have profiles which repeat periodically during propagation. Thus, it is natural to expect that in addition to the fundamental DS, one can also have HODSs in BWAs whose profiles repeat periodically during propagation. The aim of this work is to investigate the properties and dynamics of these HODSs and to compare them with HONLS solitons. This paves the way for using BWAs to simulate nonlinear extensions of the Dirac equation, as well as other solitonic and non-solitonic effects of nonlinear Dirac equations.

2. Higher-order Dirac solitons

Light propagation in a binary array of Kerr nonlinear waveguides can be described, in the continuous-wave regime, by the following dimensionless coupled-mode equation (CME) [15]:

$$i\frac{da_n(z)}{dz} = -\kappa[a_{n+1}(z) + a_{n-1}(z)] + (-1)^n\sigma a_n - \gamma|a_n(z)|^2 a_n(z), \qquad (1)$$

where a_n is the electric field amplitude in the nth waveguide, z is the longitudinal spatial coordinate, 2σ and κ are the propagation mismatch and the coupling coefficient between two adjacent waveguides of the array, respectively, and γ is the nonlinear coefficient of the waveguides. In the dimensionless form, in general, one can normalize variables in the above equation such that both γ and κ are equal to unity. However, throughout this work we will keep these parameters explicitly in Eq. (1). The form of the analytical fundamental DS solution to the CME investigated in [23] is following:

$$\begin{bmatrix} a_{2n}(z) \\ a_{2n-1}(z) \end{bmatrix} = \begin{bmatrix} i^{2n}\frac{2\kappa}{n_0\sqrt{\sigma\gamma}}\mathrm{sech}(\frac{2n}{n_0})e^{iz(\frac{2\kappa^2}{n_0^2\sigma}-\sigma)} \\ i^{2n}\frac{2\kappa^2}{n_0^2\sigma\sqrt{\sigma\gamma}}\mathrm{sech}(\frac{2n-1}{n_0})\tanh(\frac{2n-1}{n_0})e^{iz(\frac{2\kappa^2}{n_0^2\sigma}-\sigma)} \end{bmatrix}. \qquad (2)$$

It was demonstrated in [23] that with the found soliton solution in the form of Eq. (2), Eq. (1) can be converted into the nonlinear relativistic 1D Dirac equation. Unlike the exact NLS soliton solution $u(\tau) = sech(\tau)$ in optical fibers, the analytical soliton solution in the form of Eq. (2) is just approximate under certain conditions [23]. This solution is an approximation of the more general exact continuum-limit solution obtained in [22], also discussed in [19]. Nevertheless, this approximate DS solution has been proved to be excellent, cause the DS with this initial profile almost completely conserves its shape during propagation [23]. This analytical fundamental DS solution in BWAs is a one-parameter family where one parameter such as soliton peak amplitude or width can be arbitrary, provided that the soliton width is large enough (the beam width parameter $n_0 \geq 3.5$, see [23] for more details). The fundamental DS solution in the form of Eq. (2) is valid in the case when γ and σ are positive. However, with this solution one can easily construct other Dirac soliton solutions for any sign of each parameter γ and σ [23].

Supposing that ψ_n is the analytical fundamental DS solution in the form of Eq. (2), we investigate the propagation of the initial beam $a_n = r\psi_n$, where $r = 2$. Of course, one can use the exact continuum-limit solution studied in [19, 22] for constructing the beam initial conditions. However, this solution is only exact in the continuum-limit regime, and thus, also approximate in the discrete model for BWAs (like the solution we use here). Moreover, one goal of this work is to show that HODSs are robust, even when the input is not the "exact". Therefore, here we use the solution given in the form of Eq. (2). In analogy to HONLS solitons, one can expect that a beam with this initial profile shows the distinguishing feature of HO solitons, i.e., its profile changes in a periodic manner during propagation. Indeed, this is the case as shown in Fig. 1. The propagation of this beam is illustrated in Fig. 1(a) where one can see that the main body of the beam changes periodically during propagation. At first, the beam is compressed in space, then after the maximum compression it broadens again, and after reaching the maximum broadening it gets compressed. The amplitude $|a_n(z)|$ is periodic in z with the period length $L = 12.6$ for the specific set of parameters used in Fig. 1. In Fig. 1(a) one can also see weak radiations emitted from the body of the beam. This radiation is relativistic *Zitterbewegung* found in BWAs [12].

Figure 1(b) shows the two components of the beam profile at odd and even waveguide positions n. The strong component with solid curves and square markers represents the field profile $|a_{2n}|$ at even waveguide positions, whereas

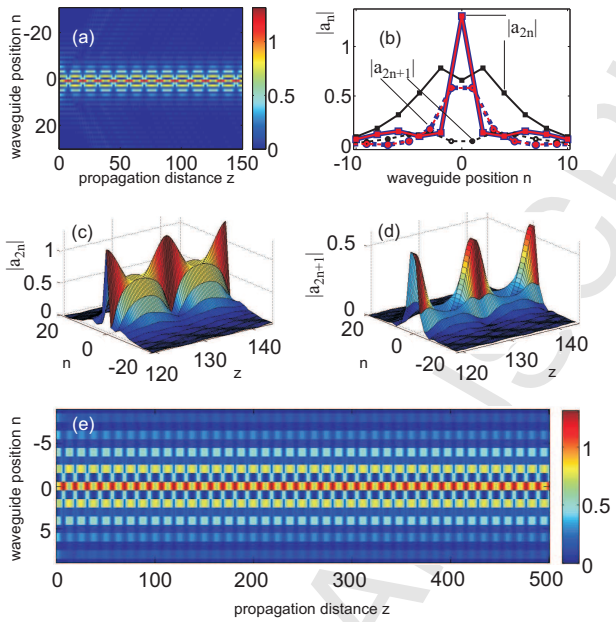

Figure 1: (Color online) (a) The propagation of a higher-order Dirac soliton with the parameter $r = 2$. (b) Profiles of the higher-order Dirac soliton at three specific propagation distances within one period: blue curves - the beginning of one period, black curves - the middle of this period, and red curves - the end of this period. (c) The propagation of intense even component $|a_{2n}|$ for two periods. (d) The propagation of weak odd component $|a_{2n+1}|$ for two periods. (e) The same as (a), but with much longer propagation distance. Parameters: κ =1; γ =1; σ = -1.2; the beam width parameter $n_0 = 5$; and the order parameter $r = 2$. The array consists of 641 waveguides.

the weak component with dashed curves and round markers represents the field profile $|a_{2n+1}|$ at odd waveguide positions. Field profiles in Fig. 1(b) are taken at three values of propagation distance within one period: $z_1 = 119.2$ (blue curves - the beginning of one period); $z_2 = z_1 + 0.5L = 125.5$ (black curves - the middle of this period); and $z_3 = z_1 + L = 131.8$ (red curves - the end of this period). One can see that the red curves (profiles at the end of one period) completely coincide with the blue curves (profiles at the beginning of this period), as a result, one can hardly see the blue curves cause they are hidden behind the red curves. Note that in Fig. 1(b) we intentionally select the greater thickness for the blue curves as compared to other curves

such that one can still recognize them behind the thinner red curves. From Figs. 1 (a) and (b) one can clearly see that at the beginning and the end of one period most of light energy is localized in the central waveguide with position $n = 0$; then during propagation the beam gradually broadens, as a result the light energy is transferred to other waveguides at two sides of the central waveguide; at the middle of this period represented by black curves in Fig. 1(b) most of light energy now is located at two waveguides with position $n = \pm 2$. Note that the initial input profile most resembles the black curves with the only significant exception that the black curve for even component $|a_{an}|$ has a dip in the center ($n = 0$), whereas the even component of the initial input curve is monotonically decaying from the center. This feature shows that the established periodic pattern is very robust and can be formed from the initial condition which is not the "exact" oscillatory solution.

In Figs. 1(c) and (d) we show the propagation of intense even component $|a_{2n}|$, and weak odd component $|a_{2n+1}|$, respectively, for *two* periods where the periodic pattern during propagation is also clearly illustrated. In Fig. 1(e) we show the propagation of the central part of the beam in Fig. 1(a), but with much longer propagation distance which exceeds any length of a BWA implementation for all current practical purposes. Our simulations show that after radiating some extra energy to the periphery of the BWA at the beginning of the propagation, the periodic regime of the beam is established over long propagation distances without any loss of energy due to radiation. So, this kind of beams can be called higher-order Dirac solitons (HODSs) in BWAs in analogy to higher-order NLS solitons in optical fibers [35, 37, 38]. Like the soliton order N for HONLS solitons, the parameter r can also be called the "order" of HODSs. It is worth noting that, like the fundamental DS in the form of Eq. (2), those HODSs also satisfy all necessary conditions to convert Eq. (1) into the nonlinear relativistic 1D Dirac equation (see [23] for more details). The total size of the BWA used for simulations in this work is large with M = 641 waveguides, and we do not impose any periodic boundary conditions in simulations such as $a_{M+1} = a_1$ as done for closed chains in [19, 20].

It is interesting to note that there are other periodic solutions to Eq. (1) which have been numerically found in [21] and termed "pulsons". By comparing the pulsons shown in Fig. 1 in [21] with the HODS shown in Fig. 1 of this work one can say that the profile of the pulson are smoother than the one of the HODS. Indeed, as shown in Fig. 1 of this work for the HODS one can see that apart from tiny regions where the spatial compression of the

HODS takes place the transverse profile of the HODS shown in Fig. 1 is like a saw blade, i.e., $|a_{2n}|$ is greater than both $|a_{2n-1}|$ and $|a_{2n+1}|$, whereas this is not the feature of the pulson. For instance, for the pulson shown in Fig. 1(a) in [21] at $t = 0$ (when the pulson is broadened) one has the following relations: $|\psi_{27}| < |\psi_{28}| < |\psi_{29}|$ and $|\psi_{33}| < |\psi_{32}| < |\psi_{31}|$. Moreover, for the broadened pulson at $t = 0$ the two symmetric peaks are located at the two neighboring sites ($n = 29$ and 31) of the center ($n = 30$), whereas for the HODS represented by the black curves in Fig. 1(b) two symmetric peaks are located at two waveguides with position $n = \pm 2$, i.e., one site farther from the center ($n = 0$) as compared to the pulson (see also Fig. 1(e)).

It is well-known that if the NLSE in optical fibers is presented in the dimensionless canonical form, then the period for HONLS solitons is $\pi/2$ in dimensionless unit where the length scale is the dispersion length $L_D = T_0^2/|\beta_2|$ with T_0 being the pulse duration and β_2 being the group velocity dispersion parameter of the fiber [35]. As mentioned above, in the case of NLS solitons in optical fibers, the true HONLS solitons have the order N which is an arbitrary integer provided that $N \geq 2$. In that case the shape of the solitons *absolutely* repeats after each period $\pi/2$. When the parameter N is not an integer, some weak radiation is emitted continuously from the body of solitons during propagation, but the shape of the central part of solitons also practically repeats after the period $\pi/2$ which is independent of the specific value of N. For HODSs, when the parameter r (which plays the role of the parameter N for HO NLS solitons) varies continuously in a certain range the main part of the solitons also repeats periodically during propagation like in the case with $r = 2$ shown in Fig. 1(a), however, the period L does depend on the specific value of r. This nontrivial feature of HODSs is illustrated in Figs. 2(a), (b), and (c) where we show their propagation with different values of the parameter $r = 1.5$, 1.8, and 2.2, respectively. All other parameters in Fig. 2 are the same as in Fig. 1. It is clear that all features in Fig. 1(a) (where the case with $r = 2$ is presented) are reproduced in Figs. 2(a), (b), and (c) (where scenarios with r not being an integer are presented) with the only exception that the period L in these Figures is different depending on the parameter r. It is important to emphasize that unlike HONLS solitons, in order to obtain HODSs in BWAs the parameter r cannot be too large, otherwise, the periodic change of the HODS amplitudes during propagation will cease to exist from the very beginning as clearly demonstrated in Fig. 2(d) where the propagation of a beam with $r = 3$ (all other parameters are also the same as in Fig. 1) is illustrated. In this case, after a certain

propagation distance [$z \simeq 20$ in Fig. 2(d)] most of light energy is just locked in the central waveguide. This feature is due to the discrete nature in WAs. It is well-known that the discreteness in WAs can create a periodic potential which is known from solid state physics as the Peierls-Nabarro (PN) potential [1]. At high powers like the case shown in Fig. 1(d) the increase of the PN potential results in a strong localization of the beam, mainly in a single waveguide which is effectively decoupled from the rest of the array. This discreteness induced effect in WAs was experimentally demonstrated in [39].

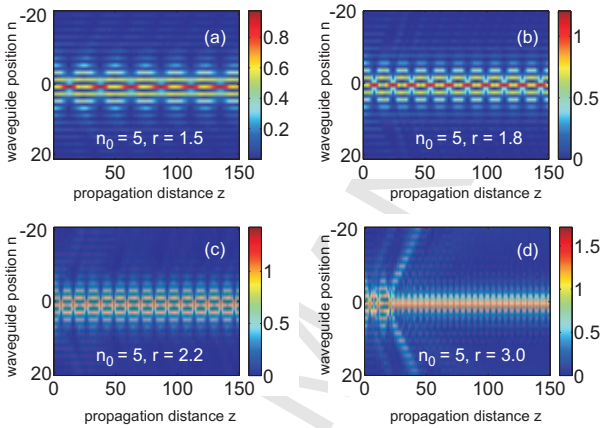

Figure 2: (Color online) (a,b,c) The propagation of higher-order Dirac solitons with the order parameter $r = 1.5$, 1.8, and 2.2, respectively. (d) The propagation of a beam with $r = 3.0$. All other parameters are exactly the same as in Fig. 1.

Now we investigate the period L of HODSs in more detail. In Figs. 3(a) and (b) we show the dependence of the period L as a function of the parameter r and σ, respectively. The green dotted, solid blue, and red dashed curves in Fig. 3(a) correspond to different values of the parameter $\sigma = 3$, 2, and 1, respectively, whereas in Fig. 3 (b) they correspond to different values of the parameter $r = 2$, 1.75, and 1.5, respectively. All other parameters are the same as in Fig. 1. It is clear from Fig. 3(a) that if the parameter r increases continuously and all other parameters are kept fixed, then the period L of HODSs will decrease. As mentioned above, this is a distinguishing feature between HODSs and HONLS solitons. The periodic change of HODS profiles also takes place for smaller values of r, provided that $r > 1$. When r gets closer to unity, the spatial broadening and compression of HODSs during propagation will be less and less pronounced. In this case, the amplitude

oscillation along the z-axis is also much weaker. Of course, when $r < 1$ the diffraction prevails over the self-focussing of the beam, and as a result, the beam will continuously broaden during propagation. In general, one can expect that the weak amplitude oscillation along the z-axis (when r is close to unity) is related to excitations of linear eigenmodes of the stationary soliton as shown in [40] for several discrete models (including the CME in the form of Eq. (1), but without the binary character, i.e., $\sigma = 0$). The full analysis of the eigenmodes of the discrete solitons/breathers for Eq. (1) when $\sigma \neq 0$ was given in [20]. However, the question as to whether HODSs with weak oscillation is associated with any of these eigenmodes analyzed in [20] is still open for discussion.

From Fig. 3(b) it is clear that if the absolute value of the parameter σ increases and all other parameters are kept fixed, then the period L of HODSs will also increase except for $|\sigma|$ in a narrow range of small values. It is worth mentioning that the analytical solution for the fundamental DS in the form of Eq. (2) is derived under condition that $|\sigma| > 2\kappa/n_0$. Therefore, one cannot use Eq. (2) to construct HODSs when $|\sigma| < 2\kappa/n_0$ (or $\sigma < 0.4$ for parameters used in this work) [23]. As a result, there is a certain lower limit (but not upper limit) for $|\sigma|$ in Fig. 3(b). This lower limit also depends on the parameter r. As mentioned above, one can always normalize variables in Eq. (1) such that both γ and κ are equal to unity. So, it is unnecessary to investigate the influence of two latter parameters on the period L.

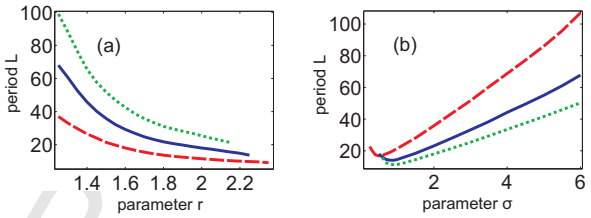

Figure 3: (Color online) (a,b) The period L as a function of the order parameters r and σ, respectively. The green dotted, solid blue, and red dashed curves in (a) correspond to different values of the parameter $\sigma = 3$, 2, and 1, respectively, whereas in (b) they correspond to different values of the parameter $r = 2$, 1.75, and 1.5, respectively. All other parameters are the same as in Fig. 1.

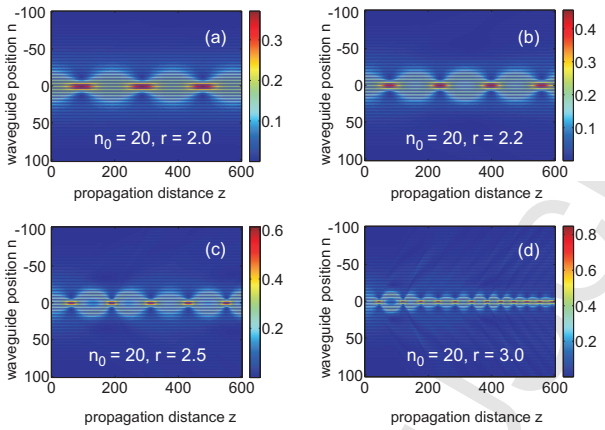

Figure 4: (Color online) (a,b,c) The propagation of higher-order Dirac solitons with the order parameter $r = 2.0$, 2.2, and 2.5, respectively. (d) The propagation of a beam with $r = 3.0$. All other parameters are exactly the same as in Fig. 2 except for a much greater width with $n_0 = 20$.

3. Discussions

A natural question is what makes HODSs different from HONLS solitons in the sense that the period of the HODSs depends substantially on the order parameter, whereas the period of the HONLS solitons remains constant. One may think that the discreteness of BWAs is the major contributing factor in this matter. It is well-known that when the beam width increases, the discreteness in WAs and BWAs will gets less and less pronounced, thus, WAs and BWAs will behave like bulk media. For instance, one can convert the coupled-mode equation governing the beam propagation in WAs (consisting of identical waveguides) into the NLSE when beam width is large enough (see how Eq. (2.5.3) is converted into Eq. (2.5.4) in [41]). Another example can be found in [42] where we show that the light bullets in WAs have the same profile as in the bulk media if the beam width is large enough. So, in order to check whether the dependence of the HODS period on the order parameter is mainly due to the discrete nature of BWAs or not, one just needs to take a much larger width (represented by the width parameter n_0) of the HODS. However, our analysis shows that this is not the case. In Fig. 4 we use $n_0 = 20$ for beam propagation simulations. By comparing Fig. 4 (where $n_0 = 20$) with Fig. 2 (where $n_0 = 5$) one can see clearly that main features of these two Figures are the same independent of the beam width:

(i) the period of HODSs decreases when the order parameter r increases and all other parameters are kept constant, (ii) when r is too large ($r = 3$) the periodicity of the beam profile is broken during propagation. Our numerical simulations with much larger n_0 (not shown here) give the same features as in Figs. 2 and 4. So, we conjecture that the binary character (represented by the parameter σ) plays the key role to make the period of HODSs depend on the order parameter. In addition, when the beam width is large enough, one can convert the CME in WAs (Eq. (1), but with $\sigma = 0$) into the NLSE as shown in [41, 42]; however, in BWAs where $\sigma \neq 0$, one can only convert Eq. (1) into the relativistic Dirac equation [23, 26], but not into the NLSE. Note also that the NLSE is integrable [35], whereas as far as we know the Dirac equation with Kerr nonlinearity is non-integrable. This fact is probably the fundamental reason why HODSs are different from HONLS solitons.

4. Conclusions

In conclusion, we investigate higher-order Dirac solitons in BWAs - optical analogues of relativistic higher-order Dirac solitons in a nonlinear extension of the 1D Dirac equation describing the dynamics of a freely moving relativistic particle. Like HONLS solitons - which are obtained from the well-known nonlinear Schrödinger equation governing the pulse propagation in an optical fiber - HODSs in BWAs have amplitude profiles which repeat periodically over large propagation distances. The main difference between HODSs and HONLS solitons is that the period of HODSs does depend substantially on the parameter r which plays the role of the order N of HONLS solitons, whereas the period of HONLS solitons does not depend on the soliton order N. We believe that the integrable nature of the NLS and the non-integrable nature of the Dirac equation with Kerr nonlinearity is the fundamental reason of this difference. In addition, the parameter r of HODSs can be any real number $r > 1$ in a certain range. The discrete nature in BWAs dictates the upper limit of this range for r in the sense that above this limit analyzed HODSs cease to exist. Our results suggest that BWAs can be used as a classical simulator to investigate not only fundamental, but also higher-order relativistic Dirac solitons.

This work is supported by the German Max Planck Society for the Advancement of Science (MPG) via the program for Max Planck Partner Groups.

References

[1] F. Lederer, G.I. Stegeman, D.N. Christodoulides, G. Assanto, M. Segev, and Y. Silberberg, Phys. Reports 463 (2008) 1.

[2] T. Pertsch, P. Dannberg, W. Elflein, A. Bräuer, and F. Lederer, Phys. Rev. Lett. 83 (1999) 4752.

[3] R. Morandotti, U. Peschel, J.S. Aitchison, H.S. Eisenberg, and Y. Silberberg, Phys. Rev. Lett. 83 (1999) 4756.

[4] M. Ghulinyan, C.J. Oton, Z. Gaburro, L. Pavesi, C. Toninelli, and D.S. Wiersma, Phys. Rev. Lett. 94 (2005) 127401.

[5] H. Trompeter, T. Pertsch, F. Lederer, D. Michaelis, U. Streppel, A. Bräuer, and U. Peschel, Phys. Rev. Lett. 96 (2006) 023901.

[6] Tr.X. Tran and F. Biancalana, Phys. Rev. Lett. 110 (2013) 113903.

[7] Tr.X. Tran and F. Biancalana, Opt. Exp. 21 (2013) 17539.

[8] Tr.X. Tran, D.C. Duong, and F. Biancalana, Phys. Rev. A 89 (2014) 013826.

[9] S. Longhi, Phys. Rev. B 81 (2010) 075102.

[10] F. Dreisow, R. Keil, A. Tünnermann, S. Nolte, S. Longhi, and A. Szameit, EPL 97 (2012) 10008.

[11] S. Longhi, Opt. Lett. 35 (2010) 235.

[12] F. Dreisow, M. Heinrich, R. Keil, A. Tünnermann, S. Nolte, S. Longhi, and A. Szameit, Phys. Rev. Lett. 105 (2010) 143902.

[13] S. Longhi, Appl. Phys. B 104 (2011) 453.

[14] J.M. Zeuner, N.K. Efremidis, R. Keil, F. Dreisow, D.N. Christodoulides, A. Tünnermann, S. Nolte, and A. Szameit, Phys. Rev. Lett. 109 (2012) 023602.

[15] A.A. Sukhorukov and Y.S. Kivshar, Opt. Lett. 27 (2002) 2112.

[16] A.A. Sukhorukov and Y.S. Kivshar, Opt. Lett. 28 (2003) 2345.

[17] M. Conforti, C. De Angelis, and T.R. Akylas, Phys. Rev. A 83 (2011) 043822.

[18] R. Morandotti, D. Mandelik, Y. Silberberg, J.S. Aitchison, M. Sorel, D.N. Christodoulides, A.A. Sukhorukov, and Y.S. Kivshar, Opt. Lett. 29 (2004) 2890.

[19] M. Johansson, K. Kirr, A.S. Kovalev, and L. Kroon, Physica Scripta 83 (2011) 065005.

[20] A. Gorbach and M. Johansson, Eur. Phys. J. D 29 (2004) 77.

[21] M. Johansson and A. Gorbach, Phys. Rev. E 70 (2004) 057604.

[22] Y.S. Kivshar and N. Flytzanis, Phys. Rev. A 46 (1992) 7972.

[23] Tr.X. Tran, S. Longhi, and F. Biancalana, Ann. Phys. 340 (2014) 179.

[24] Y. Nogami, F.M. Toyama, and Z. Zhao, J. Phys. A: Math. Gen. 28 (1995) 1413.

[25] Tr.X. Tran, X.N. Nguyen, and D.C. Duong, J. Opt. Soc. Am. B 31 (2014) 1132.

[26] Tr.X. Tran, X.N. Nguyen, and F. Biancalana, Phys. Rev. A 91 (2015) 023814.

[27] W. Heisenberg, Rev. Mod. Phys. 29 (1957) 269.

[28] D.C. Ionescu, R. Reinhardt, B. Muller, and W. Greiner, Phys. Rev. A 38 (1988) 616.

[29] A. Zecca, Internat. J. Theoret. Phys. **41,** 421-428 (2002).

[30] M.J. Esteban and E. Séré, Discrete Contin. Dyn. Syst. 8 (2002) 381.

[31] I. Bialynicki-Birula and J. Mycielski, Ann. Phys. 100 (1976) 62.

[32] N. Kemmer, Helv. Phys. Acta 10 (1937) 47.

[33] E. Fermi and C.N. Yang, Phys. Rev. 76 (1949) 1739.

[34] V.E. Zakharov and A.B Shabat, Sov. Phys. JETP 34 (1972) 62.

[35] G.P. Agrawal, *Nonlinear Fiber Optics*, 5th ed. (Academic, 2013).

[36] Y.S. Kivshar and G.P. Agrawal, *Optical Solitons: from Fiber to Photonic Crystals*, 5th ed. (Academic, 2003).

[37] H. A. Haus and M. N. Islam, IEEE J. Quantum Electron. 21 (1985) 1172.

[38] J. Satsuma and N. Yajima, Prog. Theor. Phys. Suppl. 55 (1974) 284.

[39] R. Morandotti, U. Peschel, J.S. Aitchison, H.S. Eisenberg, and Y. Silberberg, Phys. Rev. Lett. 83 (1999) 2726.

[40] P.G. Kevrekidis and M.I. Weinstein, Math. Comput. Simul. 62 (2003) 65.

[41] G.P. Agrawal, *Applications of Nonlinear Fiber Optics*, 2nd ed. (Academic, 2008).

[42] Tr.X. Tran, D.C. Duong, and F. Biancalana, Phys. Rev. A 90 (2014) 023857.